Nanoscale Advances

ROYAL SOCIETY OF CHEMISTRY

PAPER

View Article Online
View Journal | View Issue

Cite this: *Nanoscale Adv.*, 2020, **2**, 4482

Coaxial double helix structured fiber-based triboelectric nanogenerator for effectively harvesting mechanical energy†

Jinmei Liu,[a] Nuanyang Cui,[a] Tao Du,[a] Gaoda Li,[b] Shuhai Liu,[b] Qi Xu,[a] Zheng Wang,[a] Long Gu*[a] and Yong Qin*[b]

Harvesting energy from the surrounding environment, particularly from human body motions, is an effective way to provide sustainable electricity for low-power mobile and portable electronics. To get adapted to the human body and its motions, we report a new fiber-based triboelectric nanogenerator (FTNG) with a coaxial double helix structure, which is appropriate for collecting mechanical energy in different forms. With a small displacement (10 mm at 1.8 Hz), this FTNG could output 850.20 mV voltage and 0.66 mA m^{-2} current density in the lateral sliding mode, or 2.15 V voltage and 1.42 mA m^{-2} current density in the vertical separating mode. Applications onto the human body are also demonstrated: the output of 6 V and 600 nA (3 V and 300 nA) could be achieved when the FTNG was attached to a cloth (wore on a wrist). The output of FTNG was maintained after washing or long-time working. This FTNG is highly adaptable to the human body and has the potential to be a promising mobile and portable power supply for wearable electronic devices.

Received 28th June 2020
Accepted 14th August 2020

DOI: 10.1039/d0na00536c

rsc.li/nanoscale-advances

Introduction

Nowadays, mobile and portable electronics have been widely applied in communication, monitoring personal health care, monitoring environmental safety, and so on.[1–9] For powering mobile and portable electronics, numerous batteries or supercapacitors have been utilized, but their lifetime is usually limited, resulting in some problems, such as the problem of frequent charging, which greatly hinders their applications.[10–12] An effective way to solve such issues is the harvesting and utilization of the widely existing energy from the surrounding environment. In our ambient environment, numerous energy sources could be harvested and utilized, such as solar energy, mechanical energy, thermal energy, and chemical energy. As a kind of mechanical energy, human body motion energy is closely related to human activities, which make it ubiquitously available in the applicable environment for mobile and portable devices. Thus, it is important to collect and convert the human body motion energy into electricity as a mobile energy source for mobile and portable electronics.

Aimed at harvesting the widely existing mechanical energy, triboelectric nanogenerators (TENGs) were invented based on triboelectrification and electrostatic induction.[13–19] Using this technology, many groups have developed lots of wearable TENGs to harvest and convert human body motion energy into electricity,[20–35] which makes the body motion energy a feasible and available power source for mobile and portable electronics. Because of fiber's merits of being small, lightweight, bendable, and washable property, the fiber-based wearable TENGs have been widely studied.[36–38] Zhong *et al.* fabricated a fiber-based TENG to convert the biomechanical motions/vibration energy into electricity using one CNT-coated cotton fiber, and one PTFE and CNT-coated cotton fiber in an entangled structure.[39] Kim *et al.* fabricated a fabric-based TENG for powering wearable electronics by weaving fibers consisting of Al fibers and PDMS tubes.[40] Zhao *et al.* developed a wearable TENG by directly weaving Cu-coated PE fibers and polyimide-coated Cu-PET fibers in two vertical directions.[41] Dong *et al.* developed a 3-dimensional TENG for harvesting biomechanical energy using three types of fibers: blended fiber consisting of stainless steel fiber and polyester fiber, PDMS-coated energy-harvesting fiber, and binding fibers in three directions.[42] Wen *et al.* demonstrated a TENG built using a Cu-coated-EVA tube along with PDMS and Cu-coated EVA tube to collect random body motion energies.[43] After that, He *et al.* fabricated a fiber-based TENG with a silicone rubber fiber, in which the CNT layer and the copper fiber function as two electrodes.[44] Chen *et al.* reported a wearable TENG from commercial PTFE, carbon, and cotton fibers with the traditional shuttle weaving technology.[45] By

[a]*School of Advanced Materials and Nanotechnology, Xidian University, Xi'an 710071, China*

[b]*Institute of Nanoscience and Nanotechnology, Lanzhou University, Lanzhou 730000, China. E-mail: qinyong@lzu.edu.cn*

† Electronic supplementary information (ESI) available: Additional figures, including schematic diagram illustrating the fabricating process of FTNG, structure and working process of the FTNG under lateral sliding mode and vertical contact-separation mode, output performance, and the ESI videos (washing video, wearing video, whirligig video). See DOI: 10.1039/d0na00536c

choosing and processing materials together with designing a flexible structure, the fiber-based TENGs in all the above-mentioned studies can effectively scavenge mechanical energy in different forms. However, the complexity and fragility of the hybrid composites composed of cotton thread, carbon nanotube, PDMS, *etc.* could reduce their robustness and lead to disconnection or short-circuits, and further affect the output performance. Being an important factor in affecting the TENG's capacity in practical applications, it is attractive to implement a highly robust fiber-based TENG with cost-effective materials and flexible structure.

Herein, we report a fiber-based triboelectric nanogenerator (FTNG) with high robustness that can effectively scavenge biomechanical energy from both weak physiological motions and vigorous behavior. In FTNG, the positive and negative triboelectric layers (Nylon and PTFE fibers) were first wrapped with their electrodes to form the two core–shell parts of FTNG, and then these two core–shell structure fibers were twined into a coaxial double helix structure FTNG. The FTNG can be worn on the human wrist or attached to the cloth to harvest the gentle energy of body motion. Besides, it could also be used to harvest the spinning energy from a rapid rotation.

Results and discussion

As shown in Fig. 1a, FTNG consists of one Nylon fiber-wrapped Cu fiber, and one PTFE fiber-wrapped Cu fiber, and they are twined into a double helix structure. Nylon and PTFE act as the frictional surfaces and the Cu fibers present inside work as the positive and negative electrodes, respectively. The fabrication process of FTNG is illustrated in Fig. S1a† and the experimental section in detail. The optical photo of the as-fabricated FTNG shown in Fig. 1b indicates the high flexibility of this structure. An enlarged view of the part in the red square is shown in Fig. 1c, in which the Nylon/Cu fiber and PTFE/Cu fiber were interwoven at regular intervals along the axial direction. The lateral image and the cross-sectional image of FTNG are shown in Fig. S1b and c,† respectively. FTNG weighs only 0.58 g, as shown in Fig. S1d,† which demonstrates that it is light enough to be used as the wearable power source with little discomfort. Since the tensile operation is a common motion in daily activities, a tensile-loading test was essential to examine the ability of FTNG to endure mechanical operations. As shown in Fig. 1d, the composite fiber exhibits a strength of 200 MPa with a tension strain of 150%, which is a little higher than that of the Nylon-wrapped Cu fiber (~150 MPa) and PTFE-wrapped Cu fiber (~95 MPa). Moreover, a weight of 500 g can be steadily hung on the composite fiber, as shown in the inset of Fig. 1d. It can be found that the double helix structure improves the tensile property, which is beneficial for the robustness of FTNG, thereby enabling its characteristics feature of harvesting mechanical energy from violent activities.

To test the output performance of FTNG, it was tensioned by fixing its two ends, and a sewing polyester thread of 0.20 mm in

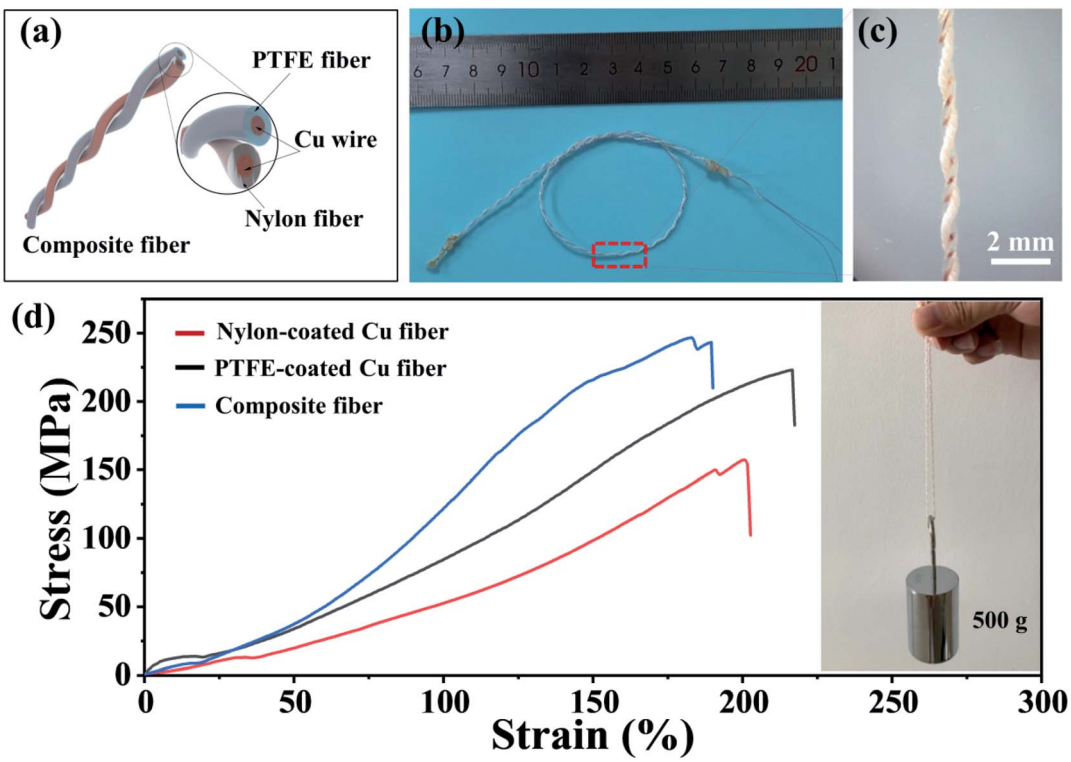

Fig. 1 (a) The structure of the FTNG. (b) Digital photography of the FTNG. (c) An enlarged view of the part marked in red square of (b). (d) Stress–strain curves of the Nylon-wrapped Cu fiber, PTFE-wrapped Cu fiber, and the composite FTNG fiber. The inset is a digital photography of the FTNG hanging a 500 g weight.

diameter as a contact object was rubbed against FTNG, as shown in Fig. S1e.† When sliding and contacting occurred, FTNG starts to work and generates electricity. Fig. 2a shows a full working cycle of the FTNG's operation in the sliding mode. When the polyester fiber moves towards the Nylon fiber, the surfaces of the two fibers come in contact and rub against each other. On the basis of the frictional series, the gaining electron's ability of polyester was relatively stronger than that of Nylon due to which electrons migrated from the Nylon surface to the polyester surface, resulting in polyester and Nylon with negative and positive charges, respectively. As displayed in Stage I, when the polyester fiber moves to the right, the contact surface between polyester and PTFE rubs against each other, and then the electrons migrate from polyester to PTFE, making the PTFE fiber a negatively charged surface. Meanwhile, the net reduced electric field drives electrons from the PTFE's electrode to the Nylon's electrode until the net electric field gets shielded by the induced charges moving from two electrodes. As shown in Stage II, when the polyester wire continues sliding to the right, the contact stage comes to the aligned position, where the positive and negative triboelectric charges were completely balanced. In the case of polyester wire sliding towards left, the contact position goes back to the misaligned condition, with the free electrons being driven from the Nylon's electrode to the PTFE's electrode, as presented in Stage III, leading to the backflow of induced free electrons. This process continues until the polyester wire keeps sliding towards the left in an aligned position (Stage IV). However, when the leftward sliding continues in a misaligned position, a reversed flow of induced electrons was observed (Stage V). Consequently, the power generation process of FTNG in one cycle was completed. By sliding the polyester fiber back and forth along the FTNG, charges got alternately transferred between the two electrodes of Nylon and PTFE. Under a 10 mm displacement at 1.8 Hz, FTNG generates an output voltage and output current of 850.20 mV and 19.52 nA, as shown in Fig. S1f and g,† respectively. An enlarged view of the output voltage peak in one cycle is shown in Fig. 2b, from which the four working stages could be observed clearly. As demonstrated in Fig. 2c, the current density could reach 0.66 mA m^{-2}, which is the ratio of the output current value and the sliding contact area. The actual contact area, here in the sliding process, was about 29.41 mm^2, which is demonstrated in detail in Table 1 in ESI.† Fig. 2d is the integral curve of the output current curve from which the accumulative charge quantity reaches 16.73 nC, and the charging rate reaches 1.67 nC s^{-1}. Here, the charging rate is an average electric quantity in one second calculated from the integral value of the current curves.

The moving speed and frictional area can largely affect the TENG's output performance. As shown in Fig. 3a and b, with a constant 10 mm sliding displacement, both the FTNG's output voltage and its output current increase with an increase

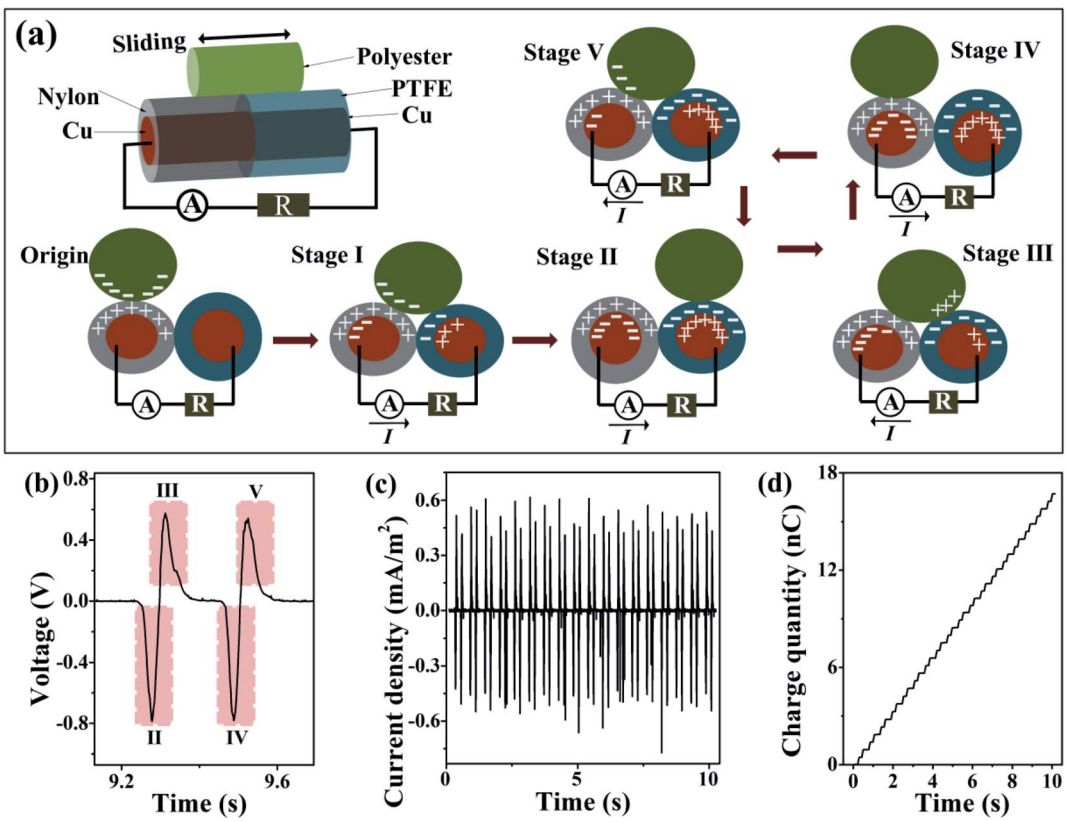

Fig. 2 (a) Working mechanism of the FTNG under a lateral sliding mode. (b) Enlarged output voltage of the FTNG a under frequency of 1.8 Hz with the displacement of 10 mm. (c) The current density of FTNG *via* dividing the output current in Fig. S1e† by the contact area. (d) The accumulative charge quantity *via* integrating the output current in Fig. S1e.†

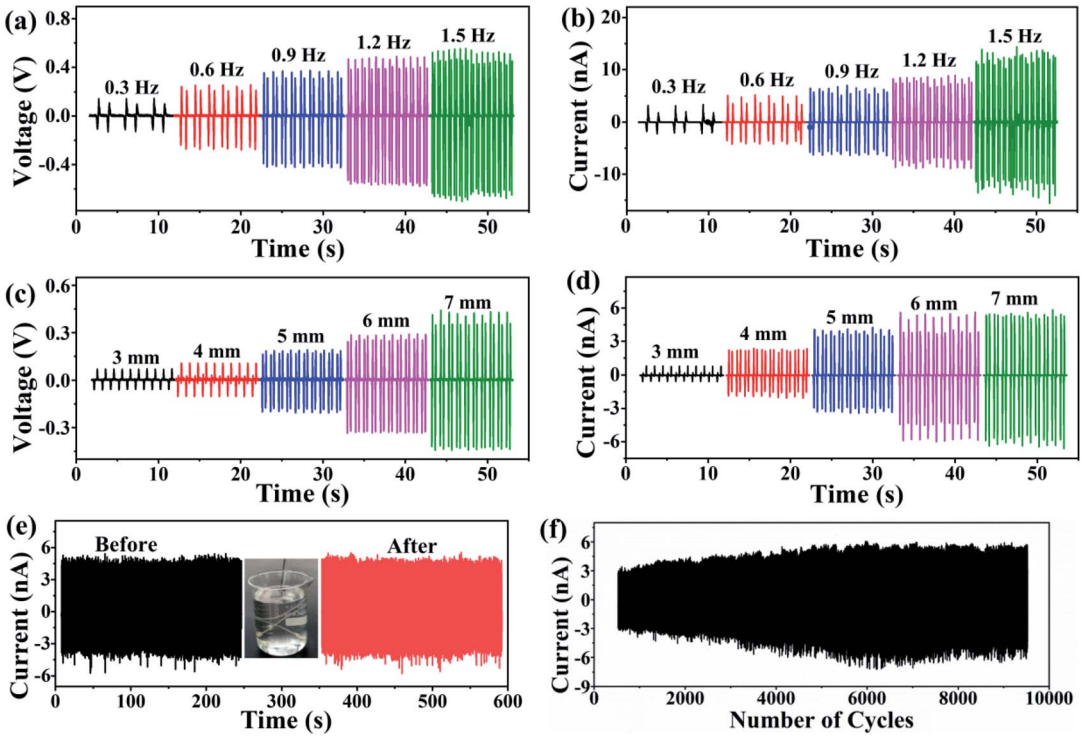

Fig. 3 (a) Output voltage and (b) output current of FTNG under different lateral sliding frequencies. (c) Output voltage and (d) output current of FTNG under different lateral sliding displacements. (e) Output current before and after washing operation. (f) Output current when continually working for 3 hours.

in the frequency. With the increase in the sliding frequency, the sliding speed becomes larger, which shortens one working cycle time and further increases the working cycle number in a fixed time. Consequently, the peak value of the open-circuit voltage increased from 140.53 mV at 0.3 Hz to 688.27 mV at 1.5 Hz (Fig. 3a). As shown in Fig. 3b, the current peak value increases from 3.13 nA at 0.3 Hz to 14.43 nA at 1.5 Hz, which means that the peak current density increases from 0.11 mA m^{-2} at 0.3 Hz to 0.48 mA m^{-2} at 1.5 Hz. During the relative sliding process, the actual frictional area between the FTNG and polyester fiber will increase with the increase in the sliding displacement. To investigate this aspect, FTNG was made to work at different sliding displacements at a fixed sliding frequency of 1 Hz. When the sliding displacement varied between 3 mm and 7 mm, the voltage peak value increased from 70.56 mV to 441.02 mV (Fig. 3c). Moreover, the current peak value increased from 0.77 nA to 6.45 nA (Fig. 3d). When divided by the contact area of 29.41 mm^2, the peak current density increased from 0.03 mA m^{-2} at 3 mm to 0.22 mA m^{-2} at 7 mm. It can be explained by stating that the larger contact area leads to increased displacement. This measurement exhibits the FTNG's ability to scavenge mechanical energy from low frequency and small amplitude motion widely existing in daily activities of humans.

As shown in Fig. 3e and ESI Video S1,† FTNG was immersed in water and stirred by a glass rod to test if FTNG can be washed like the clothes without a reduction in the performance. The comparison of the output currents before and after the washing process (Fig. 3e) shows no obvious reduction, which indicates that FTNG possesses good washing durability. Further, the robustness of FTNG was tested by continuously working for 3 h (~10 000 times) at 1 Hz sliding frequency and 10 mm sliding displacement. As shown in Fig. 3f, after the charge accumulation process, the output current remains stable, which indicates the high robustness and long-term stability of FTNG.

Aside from harvesting the sliding mechanical energy along the fiber's length direction in the above sliding mode, FTNG could also harvest the mechanical energy when it contacts and separates with other fabrics such as polyester fabric, as shown in Fig. S2a† in a contact-separating TENG working mode. As FTNG contacts and separates with the fabric, the electrons flow back-and-forth between the two electrodes in an external circuit, generating an alternating current output. Here, the polyester fabric, having fibers of 0.20 mm in diameter, was used to contact and separate with FTNG. At 1.8 Hz frequency and 20 mm displacement, the output voltage of 2.15 V and output current of 69.3 nA were achieved (Fig. S2b and c†). The corresponding peak output current density was 1.42 mA m^{-2}. The actual contact area, here in the vertical separating process, was about 48.80 mm^2, which is demonstrated in detail in Table 2 in the ESI.† The effect of the separation frequency on the FTNG's output performance was investigated with the separating distance being set at 10 mm. As shown in Fig. S2d and e,† when the frequency increases from 0.3 to 1.5 Hz, the output voltage and current increase from 436.78 mV, 4.97 nA to 1291.83 mV, 22.05 nA, respectively. Also, the corresponding current density, which can be obtained by dividing with the contact area of 48.80

mm^2, increases from 0.10 mA m^{-2} at 0.3 Hz to 0.47 mA m^{-2} at 1.5 Hz.

To test the ability of harvesting energy from the human activity, 3 FTNGs were woven into a bracelet in a parallel manner, and placed on one experimenter's wrist, as presented in Fig. 4a and ESI Video S2.† In this case, the friction occurs between FTNG and the wrist from shaking hands. Fig. 4b and c show the corresponding output voltage and output current generated by the experimenter's hand shaking motion. The output signals easily reach to 3 V and 200 nA (the enlarged view of output signals is shown in Fig. S3†). Then, 7 FTNGs were attached to the waist of one experimenter in parallel, as shown in Fig. 4d and ESI Video S3.† When the experimenter swings his arm alternately along the lateral direction and vertical direction, the friction occurs between FTNG and clothes. Fig. 4e and f show the output voltage and output current generated by the swing-arm movements, respectively. The output signals easily reach to 6 V and 600 nA, and every wave packet in them corresponds to one arm swing. The enlarged view of the output signals can be found in Fig. S4.† Therefore, this FTNG has the potential to act as a mobile and portable power supply for wearable devices.

To further test the adaptability of FTNG for versatile mechanical energy harvesting, a whirligig is used to drive FTNG. The whirligig is a circular disc that spins when pulling on strings passes through its center (radius of the central disc was ~35 mm). As shown in Fig. 5a, two FTNGs are inserted into the two center holes, respectively. The one cycle movement of the

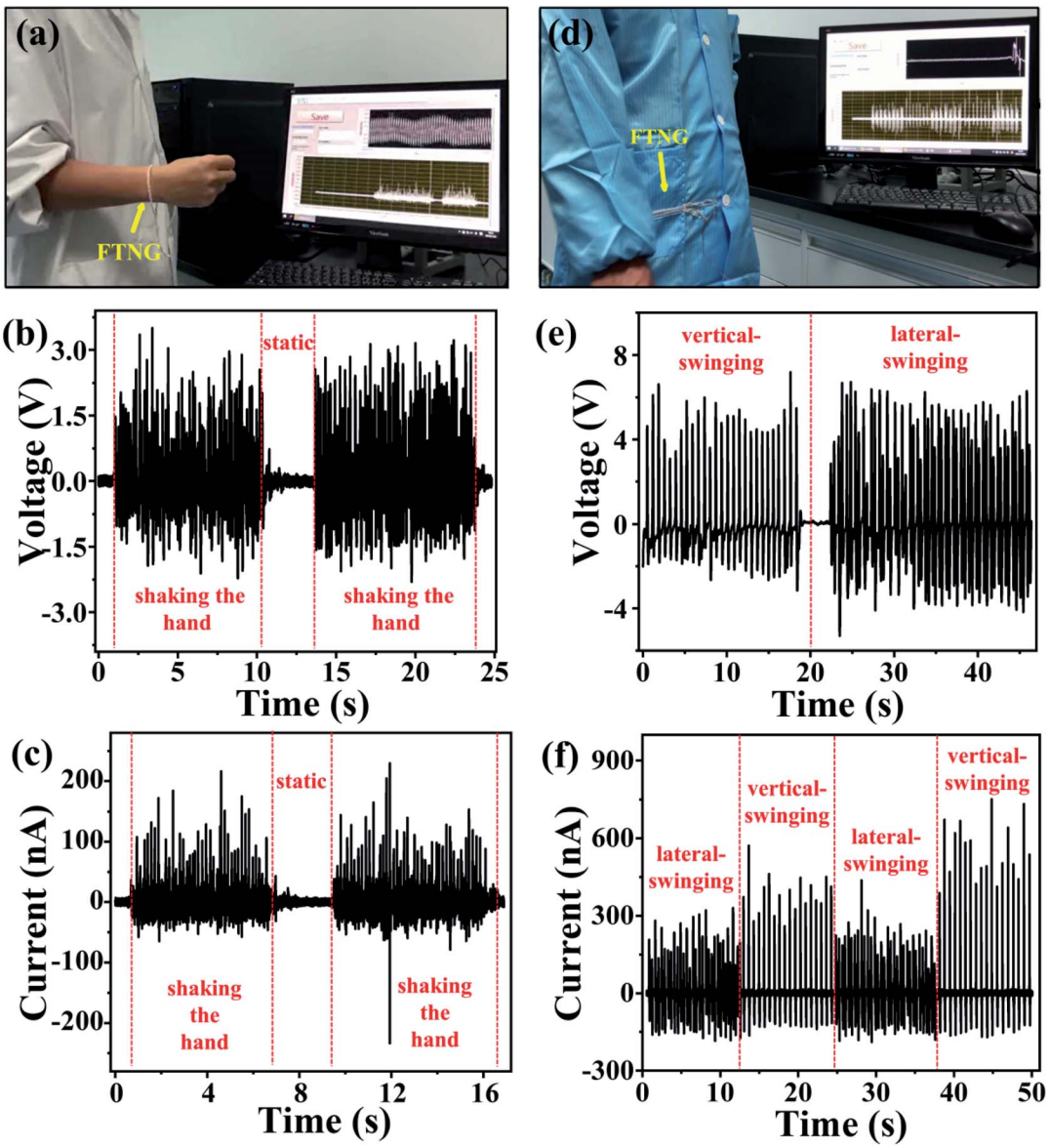

Fig. 4 (a) Demonstration of the application of FTNG to harvest the wrist motion energy. (b) Output voltage and (c) output current of FTNG driven by the wrist's motion. (d) Photograph showing the application of FTNG attached on the cloth to harvest the body motion energy in walking or jogging. (e) Output voltage and (f) output current of FTNG attached on the cloth.

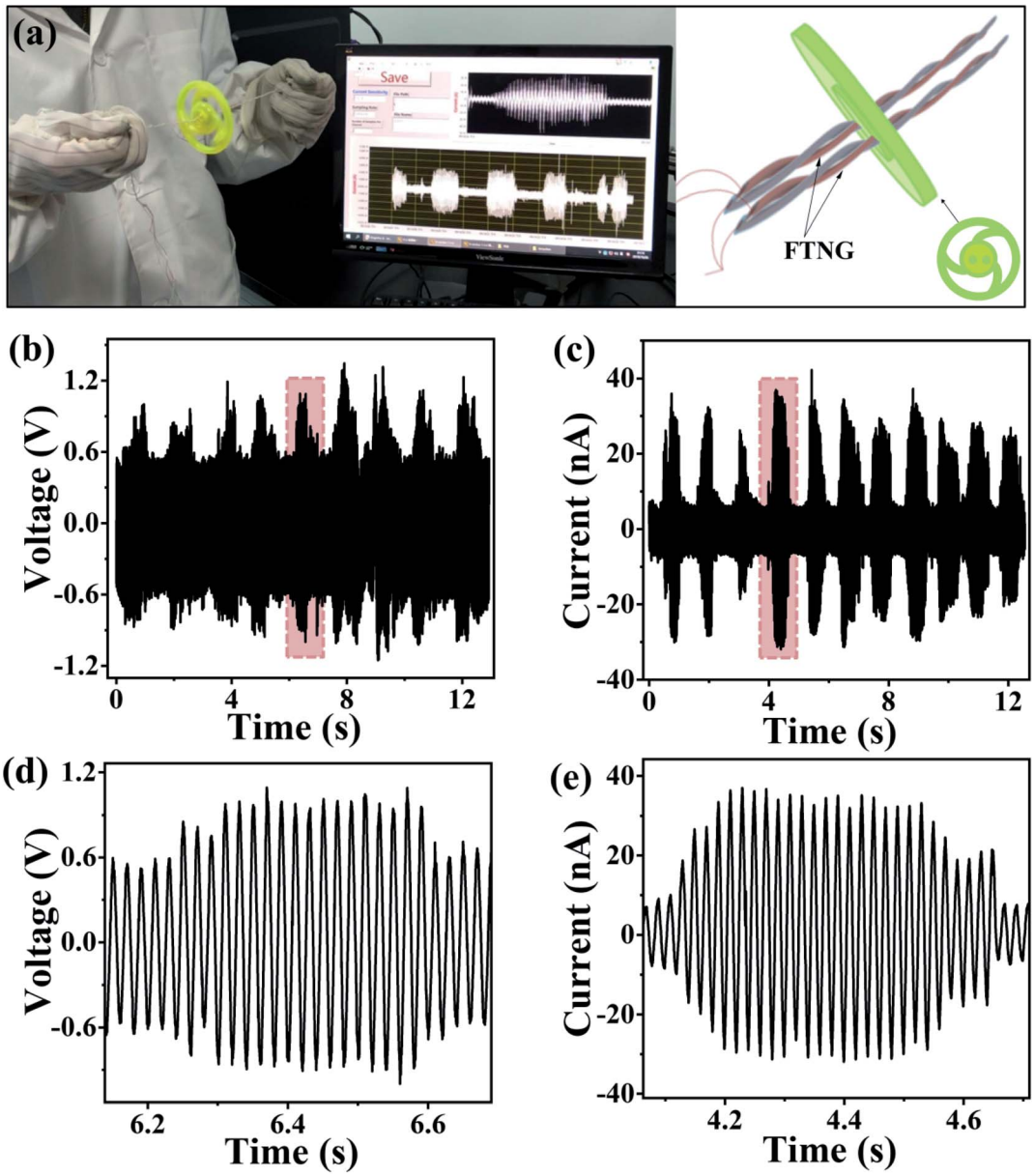

Fig. 5 (a) Schematic of the application of FTNG on harvesting the spinning energy. (b) Output voltage and (c) output current of FTNG driven by the spinning movement. The corresponding enlarged view for one wave packet of the output voltage (d) and output current (e).

circular disc consists of two processes of forward and backward windings (ESI Video S4†). During the forward winding process, the input stretching force on FTNG (exerted by the human hands) accelerates the circular disc to its maximum rotating speed. Simultaneously, the two FTNGs begin to come in contact with each other and reach a tightly coiled state. Then, in the back winding process, no input force was on the FTNG due to which the disc rotates in the reverse direction. Consequently, the two FTNGs separate from each other and get into a parallel state. After this position, the inward force was applied again, and the two FTNGs begin to come in contact with each other again. This cycle of winding and unwinding of the FTNGs repeats itself, in which electricity is generated by the two FTNGs. Fig. 5b and c show the output voltage and current driven by the spinning of the circular disc. The corresponding voltage and current were 1.2 V and 40 nA, respectively. The enlarged view of one wave packet of the output voltage and current is shown in Fig. 5d and e, respectively, which corresponds to a winding or unwinding process. This demonstration implies that such a tough FTNG can also be extended to harvest the motion energy from the high-speed and vigorous movements.

Conclusions

In summary, we developed a FTNG with a coaxial double helix structure that utilizes the general Nylon/Cu fiber and PTFE/Cu fiber for effectively harvesting the mechanical energy from the human body. Under a small displacement (10 mm, 1.8 Hz), this

FTNG could output voltage of 850.20 mV and current density of 0.66 mA m^{-2} in the lateral sliding mode, and 2.15 V and 1.42 mA m^{-2} in the vertical separating mode. Even after a washing process or a 3 hours continuous working (~10 000 cycles), no observable output performance's degradation was found. The large output of FTNG and its properties of being flexible, light-weighted, and robust structure make it suitable for continuous power harvesting. When the FTNG was worn on a human wrist, it delivered an output of 3 V voltage and 200 nA current *via* shaking hands. It can also harvest the energy in swing arms during walking and generates an output of 6 V voltage and 600 nA current when attached to the cloth. Furthermore, this FTNG is highly adaptable for harvesting the rotating mechanical energy. These features make this FTNG a promising mobile and portable power supply for wearable electronic devices.

Methods

Fabrication of the FTNG

Here, an enameled Cu wire (0.14 mm in diameter) was chosen as the inner electrode, and Nylon fibers (0.15 mm in diameter) and PTFE fibers (0.25 mm in diameter) were chosen as the frictional surface materials. At first, the Cu wire was fixed in the middle and then was wrapped by Nylon fibers to fabricate the Nylon-coated Cu fiber in the core–shell structure using a homemade rotating support. The diameter of this core–shell composite fiber was about 0.65 mm. Further, using the same method, PTFE fibers were twined around the central Cu wire to fabricate the PTFE-wrapped Cu fiber with the core–shell structure. The diameter of this fabricated fiber was about 0.72 mm. At last, the Nylon-wrapped Cu fiber and PTFE-wrapped Cu fiber were twinned with each other to form a composite fiber with a double helix structure. At last, a FTNG of 1.22 mm in diameter was formed.

Measurement of FTNG

During the output performance test of FTNG, a commercial linear motor was used to apply the external force through stretching and releasing operations. The low-noise current preamplifier SR570 was used to measure the FTNG's output current, and the low-noise preamplifier SR560 was used to measure the FTNG's output voltage.

Author contributions

The manuscript was written through contributions of all authors. All authors have given approval to the final version of the manuscript.

Conflicts of interest

There are no conflicts to declare.

Acknowledgements

Research was supported by Joint fund of Equipment Pre-Research and Ministry of Education (6141A02022518), the Fundamental Research Funds for the Central Universities (No. XJS191401, JB191403, JB191401, JB191407, no. lzujbky-2018-ot04), the National Natural Science Foundation of Shaanxi Province (NO. 2018JQ5153, 2020JM-182).

References

1 D. Son, J. Lee, S. Qiao, R. Ghaffari, J. Kim, J. E. Lee, C. Song, S. J. Kim, D. J. Lee, S. W. Jun, S. Yang, M. Park, J. Shin, K. Do, M. Lee, K. Kang, C. S. Hwang, N. Lu, T. Hyeon and D. H. Kim, Multifunctional Wearable Devices for Diagnosis and Therapy of Movement Disorders, *Nat. Nanotechnol.*, 2014, **9**, 397–404.

2 D. M. Zhang and Q. J. Liu, Biosensors and Bioelectronics on Smartphone for Portable Biochemical Detection, *Biosens. Bioelectron.*, 2016, **75**, 273–284.

3 H. Y. Guo, M.-H. Yeh, Y.-C. Lai, Y. L. Zi, C. S. Wu, Z. Wen, C. G. Hu and Z. L. Wang, All-in-One Shape-Adaptive Self-Charging Power Package for Wearable Electronics, *ACS Nano*, 2016, **10**, 10580–10588.

4 K. Deshmukh, M. B. Ahamed, K. K. Sadasivuni, D. Ponnamma, M. A. A. AlMaadeed, S. K. K. Pasha, R. R. Deshmukh and K. Chidambaram, Graphene Oxide Reinforced Poly(4-styrenesulfonic acid)/Polyvinyl Alcohol Blend Composites with Enhanced Dielectric Properties for Portable and Flexible Electronics, *Mater. Chem. Phys.*, 2017, **186**, 188–201.

5 A. Scalia, F. Bella, A. Lamber-ti, S. Bianco, C. Gerbaldi, E. Tresso and C. F. Pirri, A Flexible and Portable Powerpack by Solid-State Supercapacitor and Dye-Sensitized Solar Cell Integration, *J. Power Sources*, 2017, **359**, 311–321.

6 Y. H. Liu, J. Zeng, D. Han, K. Wu, B. W. Yu, S. G. Chai, F. Chen and Q. Fu, Graphene Enhanced Flexible Expanded Graphite Film with High Electric, Thermal Conductivities and EMI Shielding at Low Content, *Carbon*, 2018, **133**, 435–445.

7 Z. L. Wang, Entropy Theory of Distributed Energy for Internet of Things, *Nano Energy*, 2019, **58**, 669–672.

8 K. Dong, X. Peng and Z. L. Wang, Fiber/Fabric-Based Piezoelectric and Triboelectric Nanogenerators for Flexible/Stretchable and Wearable Electronics and Artificial Intelligence, *Adv. Mater.*, 2019, **32**, 1902549.

9 S. Hajra, S. Sahoo and R. N. P. Choudhary, Fabrication and Electrical Characterization of $(Bi_{0.49}Na_{0.49}Ba_{0.02})TiO_3$-PVDF Thin Film Composites, *J. Polym. Res.*, 2019, **26**, 14.

10 N. S. Choi, Z. Chen, S. A. Freunberger, X. Ji, Y. K. Sun, K. Amine, G. Yushin, L. F. Nazar, J. Cho and P. G. Bruce, Challenges Facing Lithium Batteries and Electrical Double-Layer Capacitors, *Angew. Chem., Int. Ed.*, 2012, **51**, 9994–10024.

11 K. Jost, G. Dion and Y. Gogotsi, Textile Energy Storage in Perspective, *J. Mater. Chem. A*, 2014, **2**, 10776–10787.

12 X. Pu, L. X. Li, H. Q. Song, C. H. Du, Z. F. Zhao, C. Y. Jiang, G. Z. Cao, W. G. Hu and Z. L. Wang, A Self-Charging Power Unit by Integration of a Textile Triboelectric

Nanogenerator and a Flexible Lithium-ion Battery for Wearable Electronics, *Adv. Mater.*, 2015, **27**, 2472–2478.

13 F. R. Fan, L. Lin, G. Zhu, W. Wu, R. Zhang and Z. L. Wang, Transparent Triboelectric Nanogenerators and Self-Powered Pressure Sensors Based on Micropatterned Plastic Films, *Nano Lett.*, 2012, **12**, 3109–3114.

14 V. Nguyen and R. S. Yang, Effect of Humidity and Pressure on the Triboelectric Nanogenerator, *Nano Energy*, 2013, **2**, 604–608.

15 Z. L. Wang, Triboelectric Nanogenerators as New Energy Technology and Self-Powered Sensors-Principles, Problems and Perspectives, *Faraday Discuss.*, 2014, **176**, 447–458.

16 G. Khandelwal, A. Chandrasekhar, N. R. Alluri, V. Vivekananthan, N. P. M. J. Raj and S. J. Kim, Trash to Energy: A Facile, Robust and Cheap Approach for Mitigating Environment Pollutant Using Household Triboelectric Nanogenerator, *Appl. Energy*, 2018, **219**, 338–349.

17 J. H. Choi, K. J. Cha, Y. Ra, M. La, S. J. Park and D. Choi, Development of a Triboelectric Nanogenerator with Enhanced Electrical Output Performance by Embedding Electrically Charged Microparticles, *Funct. Compos. Struct.*, 2019, **1**, 4.

18 M. Wang, J. L. Duan, X. Y. Yang, Y. D. Wang, Y. Y. Duan and Q. W. Tang, Interfacial Electric Field Enhanced Charge Density for Robust Triboelectric Nanogenerators by Tailoring Metal/Perovskite Schottky Junction, *Nano Energy*, 2020, **73**, 104747.

19 V. Vivekananthan, A. Chandrasekhar, N. R. Alluri, Y. Purusothaman and S. J. Kim, A Highly Reliable, Impervious and Sustainable Triboelectric Nanogenerator as a Zero-Power Consuming Active Pressure Sensor, *Nanoscale Adv.*, 2020, **2**, 746–754.

20 S. Jung, J. Lee, T. Hyeon, M. Lee and D. H. Kim, Fabric-Based Integrated Energy Devices for Wearable Activity Monitors, *Adv. Mater.*, 2014, **26**, 6329–6334.

21 T. Zhou, C. Zhang, C. B. Han, F. R. Fan, W. Tang and Z. L. Wang, Woven Structured Triboelectric Nanogenerator for Wearable Devices, *ACS Appl. Mater. Interfaces*, 2014, **6**, 14695–14701.

22 W. Seung, M. K. Gupta, K. Y. Lee, K. S. Shin, J. H. Lee, T. Y. Kim, S. Kim, J. J. Lin, J. H. Kim and S. W. Kim, Nanopatterned Textile-Based Wearable Triboelectric Nanogenerator, *ACS Nano*, 2015, **9**, 3501–3509.

23 N. Y. Cui, J. M. Liu, L. Gu, S. Bai, X. B. Chen and Y. Qin, Wearable Triboelectric Generator for Powering the Portable Electronic Devices, *ACS Appl. Mater. Interfaces*, 2015, **7**, 18225–18230.

24 J. Wang, S. M. Li, F. Yi, Y. L. Zi, J. Lin, X. F. Wang, Y. L. Xu and Z. L. Wang, Sustainably Powering Wearable Electronics Solely by Biomechanical Energy, *Nat. Commun.*, 2016, **7**, 12744.

25 F. R. Fan, W. Tang and Z. L. Wang, Flexible Nanogenerators for Energy Harvesting and Self-Powered Electronics, *Adv. Mater.*, 2016, **28**, 4283–4305.

26 X. Pu, W. X. Song, M. M. Liu, C. Y. Jiang, C. H. Du, C. Y. Jiang, X. Huang, D. C. Zou, W. G. Hu and Z. L. Wang, Wearable Power-Textiles by Integrating Fabric Triboelectric Nanogenerators and Fiber-Shaped Dye-Sensitized Solar Cells, *Adv. Energy Mater.*, 2016, 1601048.

27 X. Pu, L. X. Li, M. M. Liu, C. Y. Jiang, C. H. Du, Z. F. Zhao, W. G. Hu and Z. L. Wang, Wearable Self-Charging Power Textile Based on Flexible Yarn Supercapacitors and Fabric Nanogenerators, *Adv. Mater.*, 2016, **28**, 98–105.

28 Y. C. Lai, J. N. Deng, S. L. Zhang, S. M. Niu, H. Guo and Z. L. Wang, Extraordinarily Sensitive and Low-Voltage Operational Cloth-Based Electronic Skin for Wearable Sensing and Multifunctional Integration Uses: A Tactile-Induced Insulating-to-Conducting Transition, *Adv. Funct. Mater.*, 2016, **27**, 1604462.

29 W. Gong, C. Y. Hou, J. Zhou, Y. B. Guo, W. Zhang, Y. G. Li, Q. H. Zhang and H. Z. Wang, Continuous and Scalable Manufacture of Amphibious Energy Yarns and Textiles, *Nat. Commun.*, 2019, **10**, 868.

30 S. S. Kwak, H. J. Yoon and S. W. Kim, Textile-Based Triboelectric Nanogenerators for Self-Powered Wearable Electronics, *Adv. Funct. Mater.*, 2019, **29**, 1804533.

31 A. R. Mule, B. Dudem, S. A. Graham and J. S. Yu, Humidity Sustained Wearable Pouch-Type Triboelectric Nanogenerator for Harvesting Mechanical Energy from Human Activities, *Adv. Funct. Mater.*, 2019, **29**, 1807779.

32 Z. Liu, H. Li, B. J. Shi, Y. B. Fan, Z. L. Wang and Z. Li, Wearable and Implantable Triboelectric Nanogenerators, *Adv. Funct. Mater.*, 2019, **29**, 1808820.

33 J. M. Liu, L. Gu, N. Y. Cui, Q. Xu, Y. Qin and R. S. Yang, Fabric-Based Triboelectric Nanogenerators, *Research*, 2019, **2019**, 13.

34 J. M. Liu, L. Gu, N. Y. Cui, S. Bai, S. H. Liu, Q. Xu, Y. Qin, R. S. Yang and F. Zhou, Core–Shell Fiber-Based 2D Woven Triboelectric Nanogenerator for Effective Motion Energy Harvesting, *Nanoscale Res. Lett.*, 2019, **14**, 311.

35 L. Zhang, C. Su, L. Cheng, N. Y. Cui, L. Gu, Y. Qin, R. S. Yang and F. Zhou, Enhancing the Performance of Textile Triboelectric Nanogenerators with Oblique Microrod Arrays for Wearable Energy Harvesting, *ACS Appl. Mater. Interfaces*, 2019, **11**, 26824–26829.

36 Y. Cheng, X. Lu, K. H. Chan, R. R. Wang, Z. R. Cao, J. Sun and G. W. Ho, A Stretchable Fiber Nanogenerator for Versatile Mechanical Energy Harvesting and Self-Powered Full-Range Personal Healthcare Monitoring, *Nano Energy*, 2017, **41**, 511–518.

37 K. Dong, Y. Ch. Wang, J. N. Deng, Y. J. Dai, S. L. Zhang, H. Y. Zou, B. H. Gu, B. Z. Sun and Z. L. Wang, A Highly Stretchable and Washable All-Yarn-Based Self-Charging Knitting Power Textile Composed of Fiber Triboelectric Nanogenerators and Supercapacitors, *ACS Nano*, 2017, **11**, 9490–9499.

38 M. M. Liu, Z. F. Cong, X. Pu, W. B. Guo, T. Liu, M. Li, Y. Zhang, W. G. Hu and Z. L. Wang, High-Energy Asymmetric Supercapacitor Yarns for Self-Charging Power Textiles, *Adv. Funct. Mater.*, 2019, 1806298.

39 J. Zhong, Y. Zhang, Q. Zhong, Q. Hu, B. Hu, Z. L. Wang and J. Zhou, Fiber-Based Generator for Wearable Electronics and Mobile Medication, *ACS Nano*, 2014, **8**, 6273–6280.

40 K. N. Kim, J. S. Chun, J. W. Kim, K. Y. Lee, J.-U. Park, S.-W. Kim, Z. L. Wang and J. M. Baik, Highly Stretchable 2D Fabrics for Wearable Triboelectric Nanogenerator under Harsh Environments, *ACS Nano*, 2015, **9**, 6394–6400.

41 Z. Z. Zhao, C. Yan, Z. X. Liu, X. L. Fu, L. M. Peng, Y. F. Hu and Z. J. Zheng, Machine-Washable Textile Triboelectric Nanogenerators for Effective Human Respiratory Monitoring through Loom Weaving of Metallic Yarns, *Adv. Mater.*, 2016, **29**, 1702648.

42 K. Dong, J. N. Deng, Y. L. Zi, Y. C. H. Wang, C. H. Xu, H. Y. Zou, W. B. Ding, Y. J. Dai, B. H. Gu, B. Z. Sun and Z. L. Wang, 3D Orthogonal Woven Triboelectric Nanogenerator for Effective Biomechanical Energy Harvesting and as Self-Powered Active Motion Sensors, *Adv. Mater.*, 2017, **29**, 1702648.

43 Z. Wen, M.-H. Yeh, H. Y. Guo, J. Wang, Y. L. Zi, W. D. Xu, J. N. Deng, L. Zhu, X. Wang, C. G. Hu, L. P. Zhu, X. H. Sun and Z. L. Wang, Self-Powered Textile for Wearable Electronics by Hybridizing Fiber-Shaped Nanogenerators, Solar Cells, and Supercapacitors, *Sci. Adv.*, 2016, **2**, 1600097.

44 X. He, Y. L. Zi, H. Y. Guo, H. W. Zheng, Y. Xi, C. S. Wu, J. Wang, W. Zhang, C. H. Lu and Z. L. Wang, A Highly Stretchable Fiber-Based Triboelectric Nanogenerator for Self-Powered Wearable Electronics, *Adv. Funct. Mater.*, 2017, 1604378.

45 J. Chen, H. Y. Guo, X. J. Pu, X. Wang, Y. Xi and C. G. Hu, Traditional Weaving Craft for One-Piece Self-Charging Power Textile for Wearable Electronics, *Nano Energy*, 2018, **50**, 536–541.

